Morphology of the rectal gland of the spiny dogfish (*Squalus acanthias*) shark in response to feeding

Victoria Matey, Chris M. Wood, W. Wesley Dowd, Dietmar Kültz, and Patrick J. Walsh

Abstract: The morphology of the rectal gland was examined in spiny dogfish (*Squalus acanthias* L, 1758) sharks fasted (1 week) or 6 and 20 h postfeeding. The morphology of the fasted gland showed a pattern reflecting a dormant physiology, with thick gland capsule, thick stratified epithelium, and secretory parenchyma with tubules of small diameter and lumen. The secretory cells of the tubular epithelium were enlarged and irregularly shaped with abnormally condensed or highly vacuolized cytoplasm containing numerous lysosomes. Early-stage apoptotic cells were not uncommon. Secretory cells showed signs of low activity, e.g., mitochondria with weakly stained matrix and small cristae, poorly branched infoldings of basolateral membranes, and microvesicle-free subapical cytoplasm. All characteristics examined changed significantly upon feeding, consistent with increased salt and fluid secretion: the outer capsule muscle layer and the stratified epithelium decreased in diameter; the tubules enlarged; the secretory cells showed extensive development of the basolateral membrane, more mitochondria, and abundant apical microvesicles. Secretory cell apical surface was increased. The minor differences between morphology in 6 and 20 h postfeeding indicated that changes took place rapidly and were complete by 6 h. Our results are discussed in the context of prior studies of metabolism, proteomics, and cellular pathways of gland activation.

Résumé : Nous avons examiné la morphologie de la glande rectale chez des aiguillats communs (*Squalus acanthias* L., 1758) après un jeûne (1 semaine) ou alors 6 et 20 h après un repas. La morphologie de la glande après le jeûne présente un patron de physiologie de repos, avec une capsule glandulaire épaisse, un épithélium stratifié important et un parenchyme sécréteur avec des tubules à diamètre et à lumière de petite taille. Les cellules sécrétrices de l'épithélium tubulaire sont agrandies et de forme irrégulière avec un cytoplasme anormalement condensé ou fortement vacuolé contenant de nombreux lysosomes. Les cellules au premier stade de l'apoptose ne sont pas rares. Les cellules sécrétrices montrent des signes d'activité réduite, par ex., des mitochondries à matrice peu colorée et à crêtes petites, des membranes basolatérales avec des replis peu ramifiés et un cytoplasme subapical sans microvésicules. Toutes les caractéristiques examinées changent après l'alimentation, ce qui correspond à une sécrétion accrue de sels et de fluides : la couche musculaire externe de la capsule et l'épithélium stratifié diminuent en diamètre, les tubules s'agrandissent, les cellules sécrétrices affichent un développement considérable de leur membrane basolatérale et elles possèdent plus de mitochondries et des microvésicules apicales plus abondantes. La surface apicale des cellules sécrétrices augmente. Les différences mineures entre la morphologie 6 et 20 h après un repas indiquent que les changements se produisent rapidement et sont complétés au bout de 6 h. Nous discutons de nos résultats dans le contexte des études antérieures sur le métabolisme, de la protéomique et des voies cellulaires de l'activation de la glande.

[Traduit par la Rédaction]

Received 23 October 2008. Accepted 30 March 2009. Published on the NRC Research Press Web site at cjz.nrc.ca on 7 May 2009.

V. Matey. Department of Biology, San Diego State University, 5500 Campanile Drive, San Diego, CA 92182-4614, USA.
C.M. Wood. Department of Biology, McMaster University, 1280 Main Street West, Hamilton, ON L8S 4K1, Canada; Division of Marine Biology and Fisheries, Rosenstiel School of Marine and Atmospheric Science, University of Miami, 4600 Rickenbacker Causeway, Miami, FL 33149, USA; Bamfield Marine Sciences Centre, 100 Pachena Drive, Bamfield, BC V0R 1B0, Canada.
W.W. Dowd and D. Kültz. Department of Animal Science, University of California Davis, 1 Shields Avenue, Davis, CA 95616, USA.
P.J. Walsh.[1,2] Division of Marine Biology and Fisheries, Rosenstiel School of Marine and Atmospheric Science, University of Miami, 4600 Rickenbacker Causeway, Miami, FL 33149, USA; Bamfield Marine Sciences Centre, 100 Pachena Drive, Bamfield, BC V0R 1B0, Canada.

[1]Corresponding author (e-mail: pwalsh@uottawa.ca).
[2]Present address: Department of Biology, Centre for Advanced Research in Environmental Genomics, University of Ottawa, 30 Marie Curie, Ottawa, ON K1N 6N5, Canada.

Introduction

The elasmobranch rectal gland has been an organ of experimental interest for decades. This small, digitiform organ, located as an outpocketing of the posterior intestine, is responsible for salt secretion, is capable of secreting solutions that are approximately 0.5 mol/L "pure" NaCl, and close to being isosmotic with both blood plasma and external seawater. The gland was first identified as the major organ of salt excretion in elasmobranchs by Burger and Hess (1960) and Burger (1962). Although the cellular and molecular mechanisms of salt secretion are extremely well understood (Silva et al. 1997; Olson 1999; Anderson et al. 2007), and selected key activating molecules have been identified (e.g., C-type natriuretic peptide (CNP), vasoactive intestinal peptide (VIP), and other cAMP-mediated pathway activators such as forskolin, etc.), it is only in the past decade that interest has expanded to the in vivo activation of the gland by "natural feeding" and the role of this gland in secreting the excess salt load that accompanies large, infrequent, salt-laden meals. Feeding increases Na^+,K^+-ATPase activity in the gland (MacKenzie et al. 2002; Walsh et al. 2006), and it activates assorted metabolic enzymes in the gland (Walsh et al. 2006) and other tissues (notably the ornithine–urea cycle (O–UC) in liver and muscle; Kajimura et al. 2006). Furthermore, we have demonstrated that an "alkaline tide" (metabolic alkalosis) is produced by feeding (Wood et al. 2005, 2007*b*), that rectal gland secretion is stimulated by metabolic alkaosis both in vitro (Shuttleworth et al. 2006) and in vivo (Wood et al. 2007*c*), and that artificially induced alkaline loading and salt loading or volume expansion can activate some, but not all, of the metabolic pathways activated by natural feeding in the gland (Wood et al. 2008).

In parallel, proteomic approaches have begun to be applied to attempt to understand the common proteins or pathways involved in elasmobranch osmoregulatory tissues (Lee et al. 2006), and in particular the effects of feeding on the proteome of the gland (Dowd et al. 2008). While the latter study revealed some expected changes in the proteome upon feeding (e.g., a marked increase in levels of proteins associated with energy supply), we were surprised by the upregulation of proteins in the cytoskeletal or muscular category (e.g., tropomyosin alpha chain, transgelin; Dowd et al. 2008). This finding is of particular interest in light of the in vitro observations of Silva and Epstein (2002) that inhibitors of cytoskeletal function block activation of rectal gland secretion by CNP, but not its activation by VIP. These observations prompted us to re-examine the literature on rectal gland morphology.

Since the 1960s, the anatomy, histology, and ultrastructure of the rectal gland have been studied in some detail (for reviews see Olson 1999; Evans et al. 2004). The gland has been described as a highly vascularized and well-innervated organ composed of three concentric tissue layers: an outermost gland capsule, a middle secretory parenchyma, and an inner stratified (transitional) epithelium. The fibromuscular capsule that encompasses the entire gland contains a thin outer layer of connective tissue and an inner circumferential layer of smooth muscles (Chan and Phillips 1967; Olson 1999; Evans et al. 2004). This muscular band, composed of myocytes with high contractile properties, participates in the regulation of the rectal gland volume and, presumably, plays a role in its secretory function (Evans and Piermarini 2001). Secretory parenchyma provides concentration and excretion of salts from the gland. This tissue is arranged in thousands of radially oriented simple and branched tubules that drain into the central canal of the gland. Simple tubules, tightly packed and running parallel to each other, are located in the peripheral zone of parenchyma, and extensively branched tubules forming generations of "daughter" tubules of different size compose its central zone (Chan and Phillips 1967; Olson 1999). Branched tubules are thought to contain a greater volume of more concentrated salts than the simple ones (Newbound and O'Shea 2001).

Tubules contain a centrally located oval or roughly circular lumen and are covered by a unilayered epithelium that is composed of a single type of secretory cells (SCs). These SCs may be either "dark" or "light" forms depending on the density of their cytoplasmic matrix (Bulger 1963). SCs of the rectal gland tubular epithelium share major structural and functional characteristics with ion-transporting cells of other extrarenal organs in fish, reptiles, and birds (Schmidt-Nielsen 1959; Perry 1997; Shuttleworth and Hildebrandt 1999; Evans et al. 2005). Polarized SCs of the tubular epithelium have extremely infolded basolateral membranes bearing Na^+–K^+–ATPase, and Na^+–K^+–$2Cl^-$ cotransporters, and apical cell membranes forming short microvilli directed into the tubular lumen (Eveloff et al. 1979; Valentich et al. 1996; Zeidel et al. 2005). As in all actively ion-transporting cells, SCs are saturated by mitochondria in tightly packed clusters occupying spaces between extensions of basolateral membranes and distributed from the basal part of the cell to its apex (Ernst et al. 1980). Lateral membranes of the neighboring cells are extensively interdigitated. Apices of neighboring secretory cells are linked by tight junctions followed by desmosomes (Ernst et al. 1981; Forrest et al. 1982; Valentich et al. 1996). Shallow tight junctions are leaky for Na and considered the paracellular route for Na and fluid transport (Ernst et al. 1981; Forrest et al. 1982; Valentich et al. 1996). The subapical cytoplasm of secretory cells contains microfilaments, microtubules, and numerous microvesicles (Valentich et al. 1996). The third major component of the rectal gland, a stratified epithelium surrounding the central canal, is multilayered and is composed of numerous cell types (Newbound and O'Shea 2001). It is suggested that this tissue actively modifies the composition of the excreted rectal gland fluid (Bulger 1963, 1965).

Despite this extensive knowledge of the elasmobranch rectal gland, it has not been examined with reference to short-term changes such as what might occur between fed and unfed states. Given this gap in our knowledge and our previous proteomic results implicating cytoskeletal or morphological changes in the rectal gland's response to feeding, the present study examines the effect of feeding on rectal gland morphology in the spiny dogfish (*Squalus acanthias* L., 1758) shark.

Materials and methods

Experimental animals

Spiny dogfish shark (1.31–2.51 kg) were obtained by

trawl or hook and line in Barkley Sound, British Columbia, Canada, in May–June 2007. Animals were cared for in accordance with the principles of the Canadian Council on Animal Care, and protocols were approved by institutional animal care committees. At Bamfield Marine Sciences Centre, the fish were held for 1–3 weeks prior to experimentation in a 151 000 L circular tank served with running seawater at the experimental temperature of 12 ± 1 °C, salinity of 30‰ ± 2‰, and pH of 7.90 ± 0.15. We found that spiny dogfish sharks would not feed when held in smaller tanks or when isolated, but when held in a large group (approximately 100 fish) in this very large tank, a few spiny dogfish sharks would start feeding after about a week in captivity, and thereafter, the others would quickly learn to do so. The spiny dogfish sharks were fed freshly thawed whole Pacific hake (*Merluccius productus* (Ayres, 1855); from which the heads had been removed) at a ration of about 5% of body mass, every 4th day. Samples of food were taken, minced with a food processor, and frozen at –20 °C for later content analysis, as reported by Wood et al. (2007*b*).

Experimental design and sample processing

Some fish (fasted treatment) were removed from the large circular tank to a separate 1500 L tank 1 week before the start of an experiment, and were not fed during this separation period. Then each spiny dogfish shark was transferred to an individual 40 L polyurethane-coated wooden box (seawater flow = 1 L/min) described by Wood et al. (1995, 2005). For the fed fish treatments, 1 h after the start of feeding in the large 151 000 L circular tank as described above, fed fish were transferred to these same 40 L boxes. To be consistent with prior studies, fish were subsequently anesthetized (MS-222) at 12 h post-transfer (fasted fish) and 6 and 20 h postfeeding (fed fish) (i.e., 5 and 19 h post-transfer). Upon dissection, the presence of food in the gut was verified (fish that had not fed were omitted from the study and put to other use) and the rectal gland was removed. Sample size was 5 fish per treatment. Following dissection, the glands were sliced in half transversely with a razor blade and a portion from the middle part of each gland was further cut into 3–5 mm thick cross-sectional rings. These rings were used for light microscopy (LM), transmission microscopy (TEM), and scanning electron microscopy (SEM) and were fixed and processed as below. The remaining portions of the gland were rapidly frozen in liquid nitrogen so as to be useful for any follow-up molecular studies.

Light microscopy (LM), transmission electron microscopy (TEM), and scanning electron microscopy (SEM)

Routine histological examination was used to characterize the general structure of three major components of the rectal gland: the muscular layer of the outer capsule (Ca), the peripheral secretory parenchyma (SpP) and central secretory parenchyma (SpC), and the stratified epithelium (SE) (Fig. 1). Two full cross-sectional rings of the glands of 5 fish from each treatment were fixed in Serra's fixative, processed through an ethanol series and graded chloroform, and then embedded in paraffin. Serial thick cross-sections at 5–7 μm were cut on a microtome (Microm HM-355), mounted on glass slides, and stained with Gill's hematoxylin and eosin.

For LM analyses of the general structure of secretory cells (SCs) forming the tubular epithelium, we used tissues fixed and processed for TEM: 5–6 thin (≤1 mm) cross-sectional rings of the rectal glands of 5 fish from each treatment were cut into 4–8 parts, immediately fixed into hyperosmotic paraformaldehyde–glutaraldehyde Karnovsky's fixative at pH 7.2. Samples were then cut into small pieces and postfixed in 1% osmium tetroxide prepared in phosphate buffer. Subsequently, the fixed tissues were dehydrated in a graded ethanol–acetone series to 100% acetone and embedded in Epon epoxy resin. Serial semithin sections (1 μm) were cut in two tissue blocks from each fish with an ultramicrotome (EM-Leica microtome), mounted on glass slides, and stained with 0.5% Methylene Blue. Both thick and semithin sections of the rectal glands were examined under a Nikon Eclipse E200 compound microscope.

For TEM study of the ultrastructure of the secretory cells, ultrathin (60–70 nm) sections of two tissue blocks from 5 fish in each treatment were trimmed to maximize access to parenchymal tissue, cut with the same ultramicrotome used to prepare semithin sections, mounted on the copper grids, double stained with 2% uranyl acetate and 1% lead citrate, and examined under a Technai 12 transmission electron microscope (FEI) at the accelerating voltage of 80 kV.

Scanning electron microscopy (SEM) was used to examine the surface structure of the apices of the secretory cells: thick rings (5 mm) of rectal glands of three fish from each treatment were cut in halves and quarters, fixed as was described above, dehydrated in progressively elevated concentrations of ethanol concluding at 100%, and critical-point dried in liquid CO_2. Dried specimens were mounted flatly on the sample holders, sputter-coated with gold–palladium, and examined with a Hitachi S 2700 scanning electron microscope at the accelerating voltage of 20 kV.

Morphometry

Several major parameters of the rectal gland were measured in fish from each treatment: (1) thickness of the muscle layer of the outer capsule (LM, thick sections); (2) total number of secretory tubules and number of small and large tubules per square millimetre of the central part of secretory parenchyma (LM, thick sections); (3) diameters of the small and large tubules composing the central part of secretory parenchyma and diameters of their lumens (LM, thick sections); (4) thickness of the stratified epithelium (LM, thick sections); (5) number of degenerating and picnotic cells per 100 cells of secretory epithelium in fasted fish (LM, semithin sections); (6) size (height and width) of the secretory cells of tubular epithelium (LM, semithin sections); (7) number of mitochondria per secretory cell (TEM); and (8) number of desmosomes per junctional complex (TEM). Only cross-sections taken perpendicularly to the longitudinal axis of the gland were used for morphological analyses. A total of 50 measurements per treatment (10 on each fish) were done on the randomly selected slices for parameters 1, 3, 4, and 5 mentioned above. Thickness of muscle layer and stratified epithelium, and sizes (diameters and lumens) of small and large tubules were measured on the randomly selected thick slices under magnification × 600. The same sli-

Fig. 1. Light micrograph of the rectal gland (thick cross-section) of the spiny dogfish (*Squalus acanthias*) shark, showing the three components of the gland: the outer capsule; secretory parenchyma with peripheral zone composed of simple radially oriented tubules and central zone containing numerous branching tubules; and stratified epithelium lining the central duct lumen. Note a system of venous sinuses surrounding the lumen of the gland central duct. Ca, outer capsule of the gland; DL, central duct lumen; SE, stratified epithelium; SpC, secretory parenchyma, central zone; SpP, secretory parenchyma, peripheral zone; VS, venous sinus. Scale bar = 500 μm.

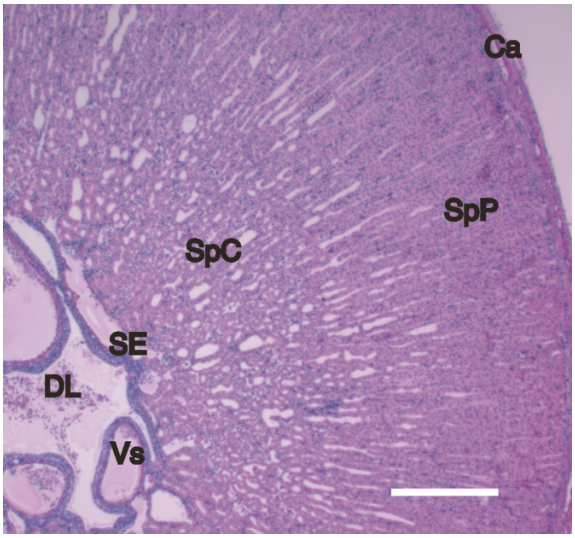

ces and magnification were used for estimation of a number of secretory tubules (5 per fish, 25 per each treatment). For determination of SC size, cells with nuclei containing visible nucleoli were randomly selected (10 per fish, 50 per each group examined) and measured under magnification × 1 500 on the randomly selected semithin slices. Number of degenerating and picnotic cells in secretory epithelia of 5 fasting fish were counted on 4 randomly selected semithin slices under magnification × 600. Number of mitochondria per secretory cells were counted in 5 fish per each treatment and ultrathin slices of 6 cells per each fish (total 30 measurements) under magnification × 2 000. Number of desmosomes per junctional complex were counted on 5 randomly selected junctional complexes per 5 fish (total 25 measurements) per each treatment under magnification × 11 500.

Statistical analysis

The replicate measures for a given sample per fish (typically 10 for each sample) were first pooled and the means obtained. These means were then further combined and subjected to statistical analysis; thus, sample size (N = 5) correctly reflects the biological variation, rather than the precision of measurement. Treatment means were compared for significance at the $p < 0.05$ level by ANOVA followed by a LSD post hoc test.

Results

Fasting spiny dogfish sharks

Histological analysis was done on three tissues composing the rectal gland in spiny dogfish sharks fasted for 1 week.

Table 1. Morphometric parameters of the rectal gland of the spiny dogfish (*Squalus acanthias*) shark under fasting conditions and 6 and 20 h postfeeding.

		Secretory parenchyma							
		Small tubules		Large tubules					
Exposure	Gland capsule (thickness of muscle layer, μm)	Diameter (μm)	Lumen (μm)	Diameter (μm)	Lumen (μm)	Total no. of tubules/mm^2	No. of small tubules/mm^2	No. of large tubules/mm^2	Stratified (epithelium thickness, μm)
Fasting	50.8±0.2a	48.5±0.6a	15.5±0.5a	107.9±1.0a	70.5±0.8a	148.8±8.6a	98.2±8.4a	50.6±6.5a	37.6±0.3a
6 h postfeeding	38.9±0.5b	62.1±0.7b	32.5±1.9b	141.2±4.0b	110.0±2.1b	151.6±6.7a	103.3±9.1a	48.4±5.2a	19.1±0.3b
20 h postfeeding	40.5±0.4b	57.8±0.7b	25.0±0.4b	134.8±1.6b	93.5±1.0b	148.1±7.7a	108.3±8.5a	40.1±4.6a	24.5±0.2c

Note: Values are means ± 1 SE (n = 5). Values sharing common letters are not significantly different between treatments ($p < 0.05$).

Fig. 2. Light micrograph of the histostructure of the outer capsule and secretory parenchyma of the rectal gland (thick cross-sections) of the fasted (A, D), 6 h postfeeding (B, E), and 20 h postfeeding (C, F) spiny dogfish (*Squalus acanthias*) shark. (A) Thick outer capsule composed of loosely packed and swollen myocytes. (B) Outer capsule showing more thin and compact muscle layer. (C) Outer capsule with compact muscle layer. (D) Central part of parenchyma composed of small and large tubules. Tubular epithelium is formed by secretory cells. (E) Enlarged small and large secretory tubules in the central part of parenchyma. Note the filamentous material within the tubule lumens. (F) Small and large secretory tubules in the central part of parenchyma. CT, connective tissue; LT, large tubule; ML, muscle layer; SC, secretory cell; SpP, secretory parenchyma, peripheral zone; ST, small tubule. Scale bars = 20 μm (A–C) and 40 μm (D–E).

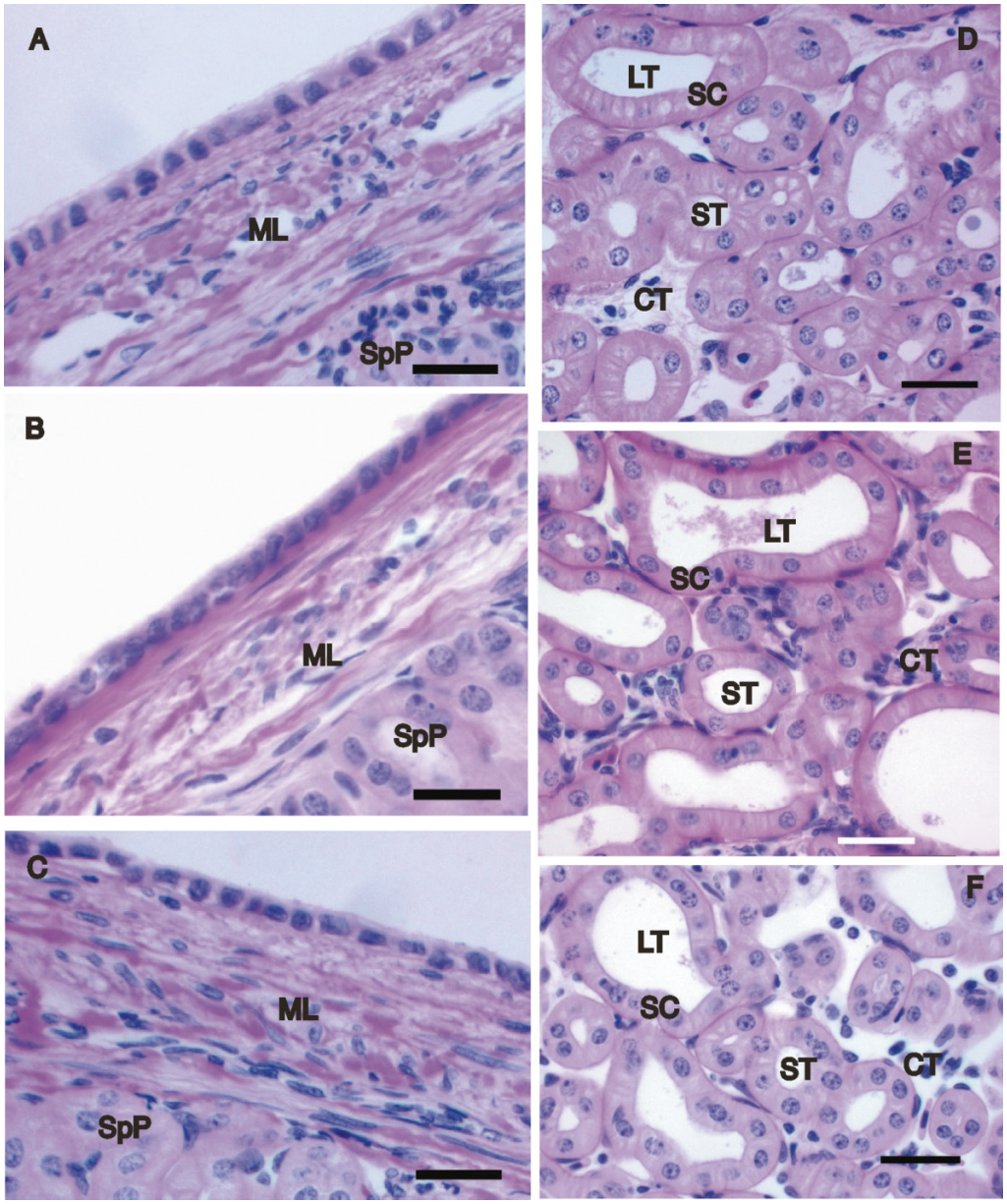

The outer capsule was thick, with a prominent muscle layer made by loosely packed and slightly swollen myocytes (Table 1; Fig. 2A). The central part of the secretory parenchyma contained numerous large and small tubules with the latter predominating (Table 1; Fig. 2D). The thick stratified epithelium was composed of 5–6 layers of enlarged cuboidal cells (Table 1; Fig. 3A).

The epithelium of both small and large tubules was almost exclusively made up of secretory cells that were highly enlarged and did not show a regular columnar shape (Table 1; Figs. 4A, 4B). Light microscopy of these cells revealed a huge and almost translucent perinuclear area containing several dense round bodies and small patch-like clusters of mitochondria associated predominantly with the basal part of the cells (Fig. 4A). TEM analysis showed that the dense bodies in the perinuclear area are lysosomes (Fig. 5A). Irregularly distributed mitochondria were seen in the middle part of the secretory cells, near labyrinth-like infoldings of lateral cell membranes (Fig. 5A). Clusters of 2–6 mitochondria were located between infoldings of basolateral membrane extended toward the perinuclear area (Fig. 5B). Mitochondria had a pale matrix and short lamellar crystae

Fig. 3. Light micrograph of the histostructure of the stratified epithelium of the rectal gland (thick cross-sections) of a fasted (A), 6 h postfeeding (B), and 20 h postfeeding (C) spiny dogfish (*Squalus acanthias*) shark. (A) Thick stratified epithelium composed of layers of cuboidal cells. (B) More thin stratified epithelium than in A. (C) Thickening of stratified epithelium. Note the mucous cells (whiteheaded arrows) in the outermost epithelial layer. DL, central duct lumen; SE, stratified epithelium; SpC, secretory parenchyma, central zone; VS, venous sinus. Scale bars = 40 μm.

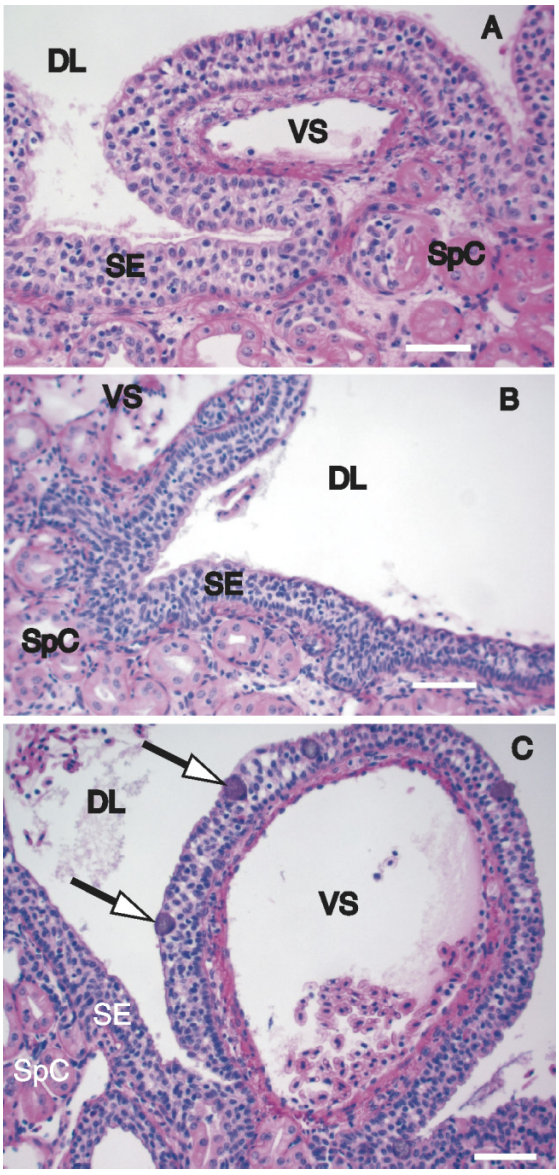

(Fig. 6A). The subapical zone of the cytoplasm contained microfilaments but was free of mitochondria or microvesicles (Fig. 6B). The apical membrane of secretory cells formed numerous irregularly shaped microvilli and some of them were fused in their basal parts (Figs. 6B, 6G). SEM showed that fused microvilli composed flower-like structures on the cell surface directed into the tubule lumen (Fig. 8A). Along with the secretory cells described above, almost 15% of cells composing tubular epithelium had regularly stained nuclei but abnormally condensed and highly vacuolized cytoplasm (Fig. 4C). About 4% of secretory cells showed signs of degeneration indicative of the early stages of apoptosis, such as a picnotic nucleus and disfigured organelles including enormously swollen mitochondria (Table 1; Fig. 7A). We also detected a few secretory cells at the advanced stages of apoptosis characterized by the formation of apoptotic bodies containing cytoplasmic material (Fig. 7B). Intercellular junctions linked apices of neighboring cells in both small and large tubules and were composed of a short tight junction followed by prominent desmosomes associated with tonofibril bundles (Figs. 5A, 6G). Fifty-two percent of complexes contained two desmosomes, and 32% and 16% contained three and one desmosomes, respectively.

Spiny dogfish sharks at 6 h postfeeding

Feeding caused dramatic changes in histo- and ultrastructures of the rectal gland. The circumferential muscle layer in the gland capsule became almost 25% thinner than in fasting fish and its myocytes were not swollen (Table 1; Fig. 2B). Total number of tubules, as well as the ratio between small and large tubules, was not changed compared with that in fasting fish but both large and small tubules became enlarged and their lumen diameters were significantly increased (Table 1; Fig. 2E). Lightly stained filamentous material was found within lumens of large and small tubules (Fig. 2E). The stratified epithelium was almost half as thick as in the fasting shiny dogfish shark and was formed by 4–5 layers of cuboidal cells (Table 1; Fig. 3B).

The tubular epithelium of both small and large tubules was formed by "dark" secretory cells that had the same shape, size, histoarchitectures, and cytoarchitectures (Figs. 2E, 4A, 4B). They were smaller than "light " secretory cells in the fasted fish, making the tubular epithelium thinner (Table 2). No degenerated cells were observed in the epithelial tissue. "Dark" secretory cells were column-shaped, with a cytoplasm of high electron density, well-developed Golgi apparati, a centrally located large nucleus, and dark strip-like clusters of mitochondria that distributed along the cells except for a narrow zone of subapical cytoplasm (Figs. 4D, 4E). The TEM study showed that this area contained abundant microvesicles and an elaborated network of microfilaments (Fig. 6D). The number of mitochondria per secretory cell was elevated almost 30% compared with that in the fasted fish (Table 2). In the apical and middle parts of the cells, they were located near the extensively interdigitated lateral membranes, and in the basal part of the cells, they were tightly packed and compressed between deep and highly branched infoldings of the basolateral membrane (Figs. 5C, 5D). In contrast to the fasted spiny dogfish sharks, mitochondria in 6 h postfeeding fish had a dense matrix and long lamellar cristae (Fig. 6C). Apical cell membranes formed numerous short and stubby microvilli covered by a well-developed glycocalyx and strengthened by microfilaments (Figs. 6D, 6H, 8B). As in fasted fish, apical junctional complexes included tight junction and desmosomes and the percentage of desmosomes per junction was not changed (Fig. 6H).

Spiny dogfish shark at 20 h postfeeding

The morphometric characteristics of the muscle layer of

Fig. 4. Light micrograph of the structure of the secretory cells of tubular epithelium (semithin cross-section) of a rectal gland of a fasted (A–C), 6 h postfeeding (D, E), and 20 h postfeeding (F, G) spiny dogfish (*Squalus acanthias*) shark showing the detailed structure of the secretory cells composing the tubular epithelium. (A, B) Part of the large and small tubules, respectively, composed of enlarged and irregularly shaped "light" secretory cells with centrally located large oval nuclei, expanded translucent perinuclear area, highly vacuolized cytoplasm, and small patch-like clusters of mitochondria (blackheaded arrows). (C) Two secretory cells showing condensed and highly vacuolized cytoplasm. (D, E) Part of large and small tubules, respectively, composed of "dark" secretory cells. Note the columnar shape of the secretory cells, dense cytoplasmic matrix, and dark strips and patches of mitochondrial clusters (blackheaded arrows) located between light bands of infolded basolateral membranes. Narrow zone of the subapical cytoplasm is less dense and shows no mitochondria. (F) Part of the large tubule composed of "light" secretory cells. Cytoplasmic matrix of low density, perinuclear and apical zones of cytoplasm have light appearance. Prominent strips of mitochondria are designated by blackheaded arrows. (G) Part of the small tubule composed by secretory cells with denser matrix of cytoplasm than in F. BL, basal lamina; CT, connective tissue; L, lumen of secretory tubule; N, nucleus; SC, secretory cell. Scale bars = 10 μm.

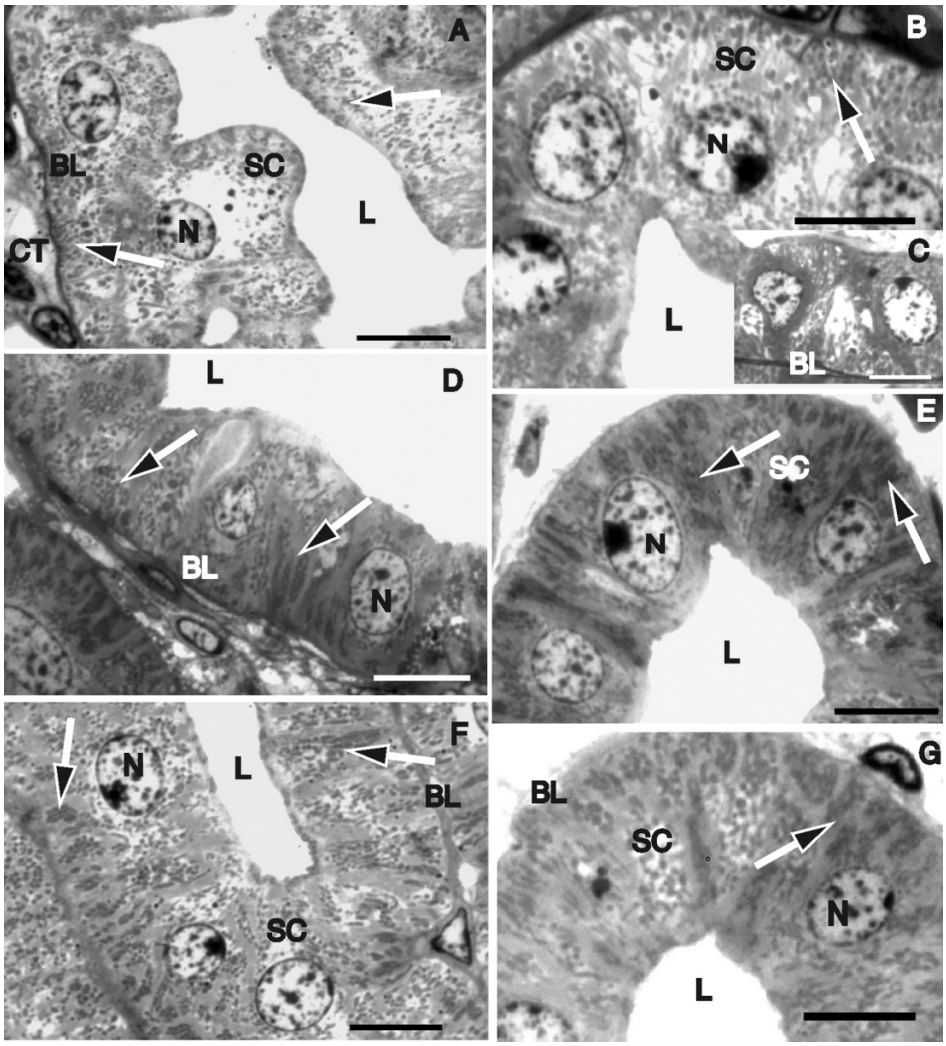

the outer capsule and the secretory parenchyma tubules did not significantly differ from those in 6 h postfeeding fish (Table 1). However, minor changes were revealed in the histostructure of the gland. The muscle layer of the capsule in 20 h postfeeding fish had a more compact appearance than in 6 h postfeeding fish (Fig. 2C). The stratified epithelium became enlarged and its outermost layer contained mucous cells (Table 1; Fig. 3C). There was a trend towards a slight increase in the number of small tubules but this trend was not significant (Table 1). Light fibrous material was seen in fewer tubules of the secretory parenchyma (Fig. 2F).

The shape and mean size of secretory cells in the tubular epithelium of the 20 h postfeeding fish was the same as in 6 h postfeeding fish (Table 2; Fig. 2F). However, some differences were found in the general structure of the epithelia and ultrastructure of the epithelial cells. In contrast with the 6 h postfeeding fish, only several tubules in the central parenchyma had an epithelium composed of the "dark" secretory cells. Epithelial tissue of the vast majority of large and small tubules was composed of the "light" cells or, more rarely, contained both "dark" and "light" secretory cells (Figs. 4F, 4G). These "dark" cells had the same structure as those found in the 6 h postfeeding fish (Fig. 4G). The "light" secretory cells were characterized by a cytoplasmic

Fig. 5. Transmission electron micrograph of the ultrastructure of the secretory cells (ultrathin longitudinal sections across secretory cells) of the tubular epithelium of the rectal gland of a fasted (A, B), 6 h postfeeding (C, D), and 20 h postfeeding (E, F) spiny dogfish (*Squalus acanthias*) shark. (A) Apical part of the cell. Cytoplasm of low electron density, huge lysosomes, enlarged mitochondria, and labyrinth-like infoldings of lateral membranes (whiteheaded arrows). The white arrow indicates apical intercellular junction. (B) Basal part of the cell. Poorly branched infoldings of basolateral membrane (blackheaded arrows) separate small clusters of weakly stained mitochondria. Basolateral membrane is underlined by invaginated supportive basal lamina. (C) Apical part of the cell. Note cytoplasm of higher electron density than in A, well-developed Golgi apparati, mitochondria, and extensively interdigitated lateral membranes forming labyrynth-like structures (whiteheaded arrows). Note intercellular junction (white arrow) and short apical microvilli. (D) Basal part of the cell. Clusters of numerous mitochondria with dense matrix are compressed between branched infoldings of basolateral membrane (blackheaded arrows). (E) Apical part of the cell. Note highly elaborated labyrinth-like infoldings of lateral membranes (whiteheaded arrows), mitochondria and light perinuclear area. (F) Basal part of the cell. Clusters of mitochondria are located between interdigitations of basolateral membranes (blackheaded arrows). Note deep invaginations of supportive basal lamina. BL, basal lamina; Ga, Golgi apparatus; LS, lysosome; M, mitochondria; N, nucleus. Scale bars = 2 μm.

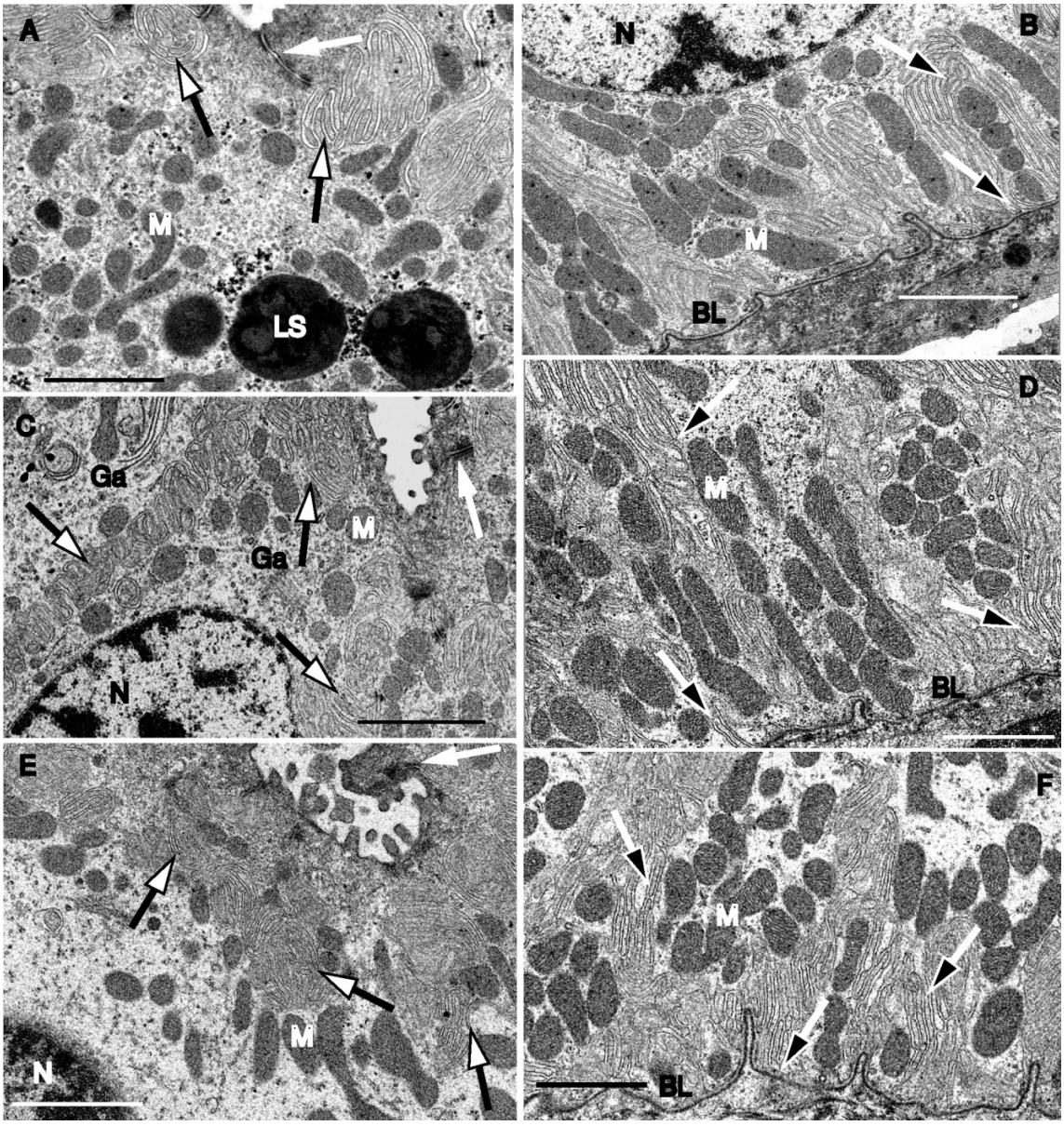

matrix of lower density and an expanded and almost translucent perinuclear zone and abundant mitochondria (Table 2; Figs. 4F, 7A, 7B). As in the "dark" cells, mitochondria exhibited a dense matrix and long cristae (Fig. 6E). They were located between deeply invaginated infoldings of basolateral membranes and in a close proximity to lateral membranes that, especially in the apical part of the cells, formed complex labyrinth-like structures and the basolateral membrane was deeply invaginated (Figs. 5E, 5F, 6E). The subapical cytoplasm of "light" cells, as well as in "dark" cells, was rich in microvesicles and microfilaments (Fig. 6F). The apical membrane in both "light" and "dark" cells formed

Fig. 6. Transmission electron micrographs showing detailed structure of the secretory cells of the tubular epithelium of the rectal gland of a fasted (A, B, G), 6 h postfeeding (C, D, H), and 20 h postfeeding (E, F, I) spiny dogfish (*Squalus acanthias*) shark. (A) Mitochondria between two sets of lateral membranes (whiteheaded arrow). Note the low electron density of the mitochondrial matrix and short lamellar cristae. (B) Apical cell membrane and subapical zone of cytoplasm. Apical cell membrane forms short microvilli. Subapical zone of cytoplasm contains microfilaments and is free of mitochondria and microvesicles. (C, E) Mitochondria between sets of lateral membrane (whiteheaded arrows) in 6 and 20 h fasting fish, respectively. Note high electron density of mitochondrial matrix and long lamellar cristae, and close association between mitochondria and highly interdigitated cell membranes. (D, F) Apical membrane and subapical zone of cytoplasm in a 6 and 20 h fasting fish, respectively. Apical membrane forms stubby microvilli in 6 h fasting fish (C) and more expended microvilli in 20 h fasting fish (F). Subapical cytoplasm of the secretory cells contains developed network of microfilaments and numerous microvesicles located in close proximity to apical membrane. (G, H, I) Apical junctional complex joining adjacent secretory cells in fasted, 6 h postfeeding, and 20 h postfeeding fish, respectively. In both fasted and postfeeding fish apical complexes include short tight junction and well-developed desmosomes associated with prominent bundles of tonofibrils (white asterisks). Note well-developed glycocalyx covering apical cell membrane in fasted and postfeeding fish (G–I) and fused microvilli in fasted fish (G). D, desmosome; M, mitochondria; Mf, microfilaments; Ms, microvesicles; Mv, microvilli; TJ, tight junction. Scale bars = 1 μm (A, C, E), 0.5 μm (B, D, F), and 0.2 μm (G, H, I).

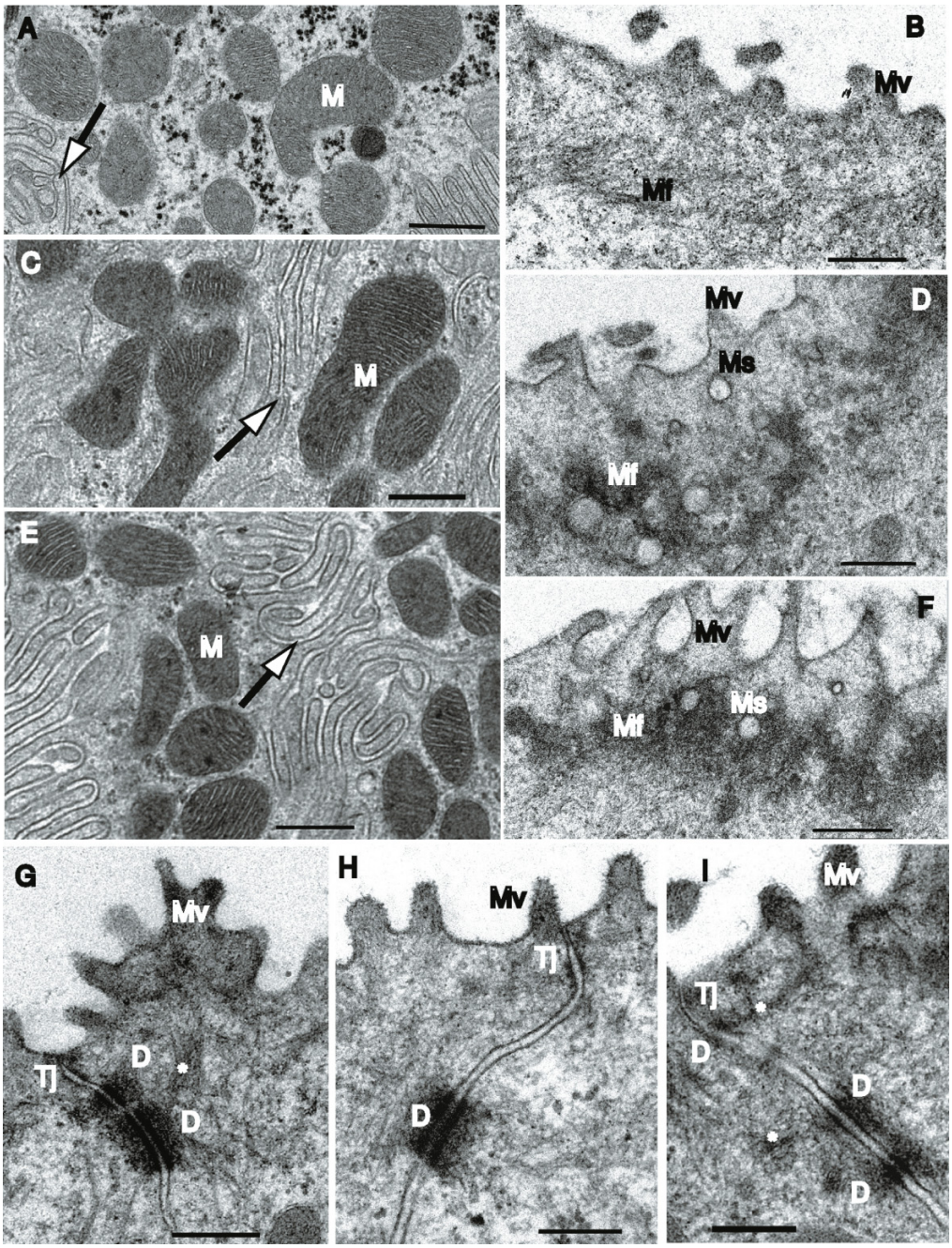

Fig. 7. Transmission electron micrographs showing degenerated secretory cells in the tubular epithelium of the rectal gland of fasted spiny dogfish (*Squalus acanthias*) shark. (A) Cell at the early stage of apoptosis. Note picnotic nucleus and enormously swollen and disfigured cell organelles. (B) Cell at the advanced stage of apoptosis with huge apoptotic body containing cytoplasmic material. In both A and B, degenerated cell is surrounded by secretory cells showing regular structure. Ab, apoptotic body; DC, degenerated cell; N, nucleus; SC, secretory cell. Scale bars = 2 μm.

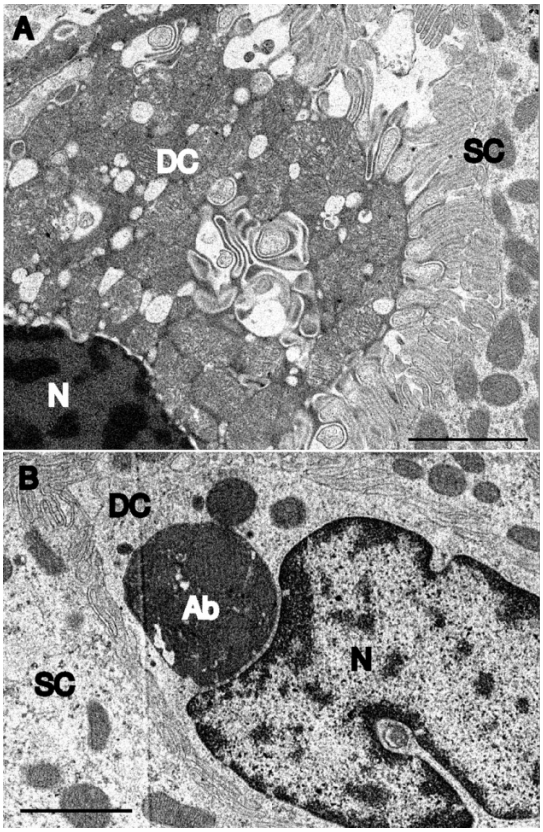

slightly expanded microvilli that showed a tendency to cluster (Figs. 5E, 6F, 8C). Ultrastructure of the apical junctional complexes between neighboring secretory cells remained unaltered (Fig. 6I).

Discussion

While the physiology of the elasmobranch rectal gland has been well studied, the morphology appears to have been characterized primarily under relatively static or singular physiological conditions. One exception is that there have been several studies of the mass of the rectal gland in the context of salinity variations showing either a general trend towards lower mass in freshwater (Oguri 1964; Piermarini and Evans 1998) or no effect of salinity (Pillans and Franklin 2004). In a recent study of freshwater- and seawater-adapted bull sharks (*Carcharhinus leucas* (Müller and Henle, 1839)), morphological structural changes in the rectal gland were limited (Pillans et al. 2008). The above studies suggest that morphological changes in the rectal gland may be less important in the adaptation to altered salinity than to changes in other physiological variables. The current study is the first to examine the morphology of the elasmobranch rectal gland under both the basal physiological activity and the naturally heightened secretory activity that follows feeding.

This study has demonstrated clearly that there are marked morphological differences between the gland in 1 week fasted sharks and the gland in 6 and 20 h postfeeding sharks. The overall impression of the morphology of the gland after 1 week of fasting is that it is relatively dormant, with a thick gland capsule, a thick stratified epithelium, and a secretory parenchyma that is composed of tubules of smaller diameter and lumen. Secretory cells of tubular epithelium were enlarged and irregularly shaped. Almost 15% of them were represented by cells undergoing degeneration, and 4% of secretory cells were at the early stages of apoptosis. Mitochondria of the secretory cells had a weakly stained matrix and small cristae, an observation that is consistent with prior observations of decreased mitochondrial activity by enzyme and protein measures (Walsh et al. 2006; Dowd et al. 2008). The absence of apical microvesicles that perform transport functions may be associated with a depressed metabolic requirement. Additionally, the apical surface of the secretory cells had a reduced relief owing to fusion of microvilli, which would effectively decrease the salt secretion surface area.

Virtually all of the morphological characteristics examined in this study changed markedly upon feeding, consistent with an increased role in salt and fluid secretion: both the muscle layer of outer capsule and stratified epithelium decreased in diameter and the tubules enlarged including an increase in tubule diameter. The secretory cells changed ultrastructure, showing charactreristics common for actively functioning ion-transporting cells such as extensive amplification of the basolateral membrane bearing Na^+–K^+–ATPase, higher populations of mitochondria with dense matrix and developed cristae, and abundant apical microvesicles (Perry 1997). The pattern of the apical surface of secretory cells was changed and SEM data clearly demonstrated increased surface area for secretion in fed fish. The stable number of desmosomes in the apical junctional complexes between secretory cells in fasted and fed fish showed that feeding or starvation did not affect the overall integrity of the epithelial tissue.

Perhaps the most surprising aspect of this study is the general similarity of the gland morphology between 6 and 20 h postfeeding, i.e., that morphological "activation" appeared to be complete within 6 h following a meal. The timing of the morphological changes are consistent with what appears to be a peak or plateau in activity of the gland and other altered physiological processes in several other studies using a similar feeding protocol. Notably, Wood et al. (2005) have shown that the alkaline tide peaks at about 6 h postfeeding, yet the activation of the base extrusion mechanism to the water at the gills is sustained well beyond 20 h postfeeding (Wood et al. 2007*c*). Several biochemical measures with a similar timing are increases in activities of isocitrate dehydrogenase (EC 1.1.1.41), citrate synthase (EC 2.3.3.1), and lactate dehydrogenase (EC 1.1.1.27) in the rectal gland (Walsh et al. 2006); increases in nitrogen metabolizing enzymes in a variety or other tissues (Kajimura et al. 2006); and patterns of plasma metabolites (Kajimura et al. 2006; Walsh et al. 2006). Changes in abundance of several

Fig. 8. Scanning electron micrograph of the structure of the apical surface of secretory cells faced into the lumen of secretory tubule of the rectal gland of the spiny dogfish (*Squalus acanthias*) shark. (A) Fusion of microvilli and formation of complex flower-like structures (whiteheaded arrows); fasting animal. (B) Short regular microvilli, 6 h postfeeding. (C) Clustering of microvilli, 20 h postfeeding. Scale bars = 2 μm.

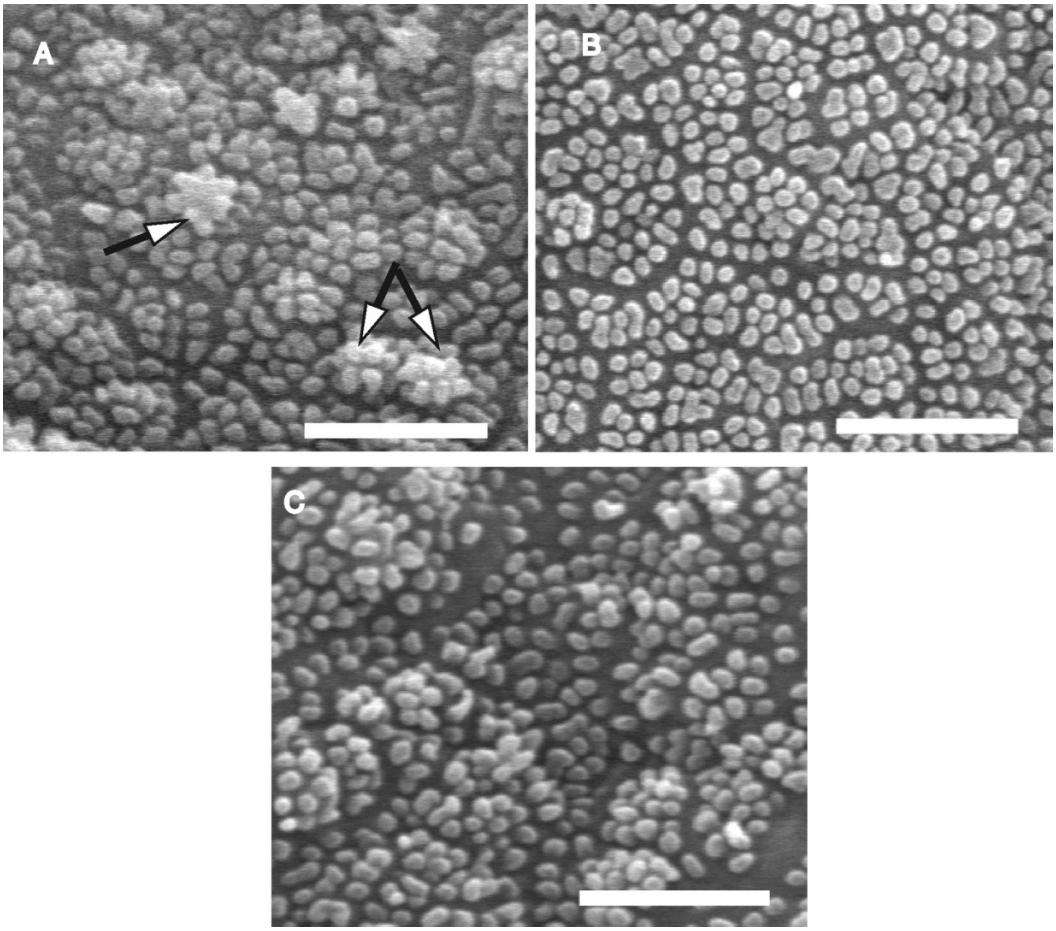

Table 2. Characteristics of the secretory cells in the rectal gland of the spiny dogfish (*Squalus acanthias*) shark under fasting conditions and 6 and 20 h postfeeding.

	Secretory cells		
Exposure	Height (μm)	Width (μm)	No. of mitochondria per cell
Fasting	18.7±0.2a	14.9±0.1a	57.9±1.8a
6 h postfeeding	14.3±0.1b	12.2±0.2b	77.0±1.6b
20 h postfeeding	13.9±0.2b	12.5±0.2b	74.6±2.1b

Note: Values are means ± 1 SE (n = 5). Values sharing common letters are not significantly different between treatments ($p < 0.05$).

proteins in the rectal gland are also completed within 6 and 20 h after a meal (Dowd et al. 2008). These included transgelin and tropomyosin alpha, both of which were upregulated following feeding. Transgelin is an actin cross-linking protein that has been implicated in the stability of the actin cytoskeleton (Goodman et al. 2003). Transgelin may be involved in smooth muscle contractile activity in the gland following feeding and (or) it could play a role in polarization of SCs, but immunocytochemical localization data from before and after feeding are needed to begin to clarify the role of this protein.

Overall, our study indicates that major, apparently coordinated morphological changes coincide with the coordinated regulation of numerous proteins involved in energy metabolism and regulation of cytoskeletal or muscular activity, in addition to several proteins whose identities and functions are currently unknown (Dowd et al. 2008). Together, these events contribute to the activation or deactivation of salt secretion upon feeding or fasting in elasmobranch rectal gland. Similar rapid and radical morphological changes have been observed in other comparative models, notably the gut of pythons (genus *Python* Daudin, 1803) (Lignot et al. 2005; Ott and Secor 2007). It will be interesting to further examine these comparative models to discover if there are general features (e.g., patterns of protein translation and activation) of tissues that go through long periods of inactivity followed by periods of very intense work associated with feeding. Furthermore, our studies have yet to identify or pinpoint the specific stimulus or stimuli and signaling pathway(s) responsible for coordinating these activating events.

While our studies have yet to identify the specific stimulus or stimuli that trigger these activating events, our morphological findings may also shed light on the signaling pathways responsible for rectal gland activation in vivo. Using an in vitro perfused gland preparation, Silva and Epstein

(2002) demonstrated that CNP activation of the gland could be blocked substantially (50%) by cytochlasin-D (an inhibitor of actin organization) and completely by ML-7 (an inhibitor of Myosin light chain kinase; EC 2.7.11.18), whereas these inhibitors of cytoskeletal or contractile elements had no effect on VIP activation of the gland. Given the rather pronounced and rapid changes in morphology of the gland that we have demonstrated following feeding, a natural activator of gland secretion, it is tempting to speculate that CNP-mediated activation is a predominant activation pathway in vivo. Comparative morphological studies of the in vitro perfused rectal gland following either CNP or VIP activation would also be interesting in this regard.

This study also demonstrates how modern molecular approaches such as proteomics can and should be juxtaposed with more classical techniques. In this case, measurements of an array of proteins suggested substantial morphological restructuring, yet these predictions could only be best tested by time-proven methodology.

Acknowledgements

P.J.W. and C.M.W. are supported by Natural Sciences and Engineering Research Council of Canada Discovery Grants and the Canada Research Chair Program. We wish to thank Bruce Cameron and all the support staff at the Bamfield Marine Sciences Centre for making possible this study. We thank Steve Barlow (San Diego State University, SDSU) for his encouragement and suggestions regarding electron microscopy and Natalie Gude (SDSU) for her valuable technical assistance in histology of the gland. W.W.D. was supported by a Coastal Environmental Quality Initiative Fellowship from the University of California Marine Council. D.K. acknowledges research support from the National Science Foundation (IOS-0542755).

References

Anderson, W.G., Taylor, J.R., Good, J.P., Hazon, N., and Grosell, M. 2007. Body fluid volume regulation in elasmobranch fish. Comp. Biochem. Physiol. Part A Mol. Integr. Physiol. **148**: 3–13. doi:10.1016/j.cbpa.2006.07.018.

Bulger, R.E. 1963. Fine structure of the rectal (salt-secreting) gland of the spiny dogfish, *Squalus acanthias*. Anat. Rec. **147**: 95–127. doi:10.1002/ar.1091470108. PMID:14062368.

Bulger, R.E. 1965. Electron microscopy of the stratified epithelium lining the excretory canal of the dogfish rectal gland. Anat. Rec. **151**: 589–607. doi:10.1002/ar.1091510410.

Burger, J.W. 1962. Further studies on the function of the rectal gland in the spiny dogfish. Physiol. Zool. **35**: 205–217.

Burger, J.W., and Hess, W.N. 1960. Function of the rectal gland in the spiny dogfish. Science (Washington, D.C.), **131**: 670–671. doi:10.1126/science.131.3401.670. PMID:13806061.

Chan, D.K., and Phillips, J.G. 1967. The anatomy, histology and histochemistry of the rectal gland in the lip-shark *Hemiscyllium plagiosum* (Bennett). J. Anat. **101**: 137–157. PMID:6047696.

Dowd, W.W., Wood, C.M., Kajimura, M., Walsh, P.J., and Kültz, D. 2008. Natural feeding influences protein expression in the dogfish shark rectal gland: a proteomic analysis. Comp. Biochem. Physiol. Part D Genomics, Proteomics, **3**: 118–127.

Ernst, S.A., Riddle, C.V., and Karnaky, K.J., Jr. 1980. Relationship between localization of Na^+K^+-ATPase, cellular fine structure and reabsorptive and secretory electrolyte transport. *In* Current topics in membranes and transport. Vol. 13. Cellular mechanisms of renal tubular ion transport. *Edited by* F. Bronner and A. Kleinzeller. Academic Press, New York. pp. 355–385.

Ernst, S.A., Hootman, S.R., Schreiber, J.H., and Riddle, C.V. 1981. Freeze-fracture and morphometric analysis of occluding junctions in rectal glands of elasmobranch fish. J. Membr. Biol. **58**: 101–114. doi:10.1007/BF01870973. PMID:6260950.

Evans, D.H., and Piermarini, P.M. 2001. Contractile properties of the elsamobranch rectal gland. J. Exp. Biol. **204**: 59–67. PMID: 11104711.

Evans, D.H., Piermarini, P.M., and Choe, K.P. 2004. Homeostasis: osmoregulation, pH regulation, and nitrogen excretion. *In* Biology of sharks and their relatives. *Edited by* J.C. Carrier, J.A. Musick, and M.R. Heithaus. CRC Press, Boca Raton, Fla. pp. 247–268.

Evans, D.H., Piermarini, P.M., and Choe, K.P. 2005. The multifunctional fish gills: dominant site of gas exchange, osmoregulation, acid–base regulation, and excretion of nitrogenous waste. Physiol. Rev. **85**: 97–177. doi:10.1152/physrev.00050.2003. PMID:15618479.

Eveloff, J., Karnaky, K.J., Jr., Silva, P., Epstein, F.H., and Kinter, W.B. 1979. Elasmobranch rectal gland cell: autoradiographic localization of [^{3}H] ouabain-sensitive Na,K-ATPase in the rectal gland of dogfish, *Squalus acanthias*. J. Cell Biol. **83**: 16–32. doi:10.1083/jcb.83.1.16. PMID:229110.

Forrest, J.N., Jr., Boyer, J.L., Ardito, T.A., Murdaugh, H.V., Jr., and Wade, J.B. 1982. Structure of tight junctions during Cl secretion in the perfused rectal gland of the dogfish shark. Am. J. Physiol. **242**: C388–C392. PMID:7081428.

Goodman, A., Goode, B.L., Matsudaira, P., and Fink, G.R. 2003. The *Saccharomyces cerevisiae* calponin/transgelin homolog Scp1 functions with fimbrin to regulate stability and organization of the actin cytoskeleton. Mol. Biol. Cell, **14**: 2617–2629. doi:10.1091/mbc.E03-01-0028. PMID:12857851.

Kajimura, M., Walsh, P.J., Mommsen, T.P., and Wood, C.M. 2006. The dogfish shark (*Squalus acanthias*) activates both hepatic and extra-hepatic ornithine urea cycle enzyme activities for nitrogen conservation after feeding. Physiol. Biochem. Zool. **79**: 602–613. doi:10.1086/501060. PMID:16691526.

Lee, J., Valkova, N., White, M.P., and Kültz, D. 2006. Proteomic identification of processes and pathways characteristic of osmoregulatory tissues in spiny dogfish shark (*Squalus acanthias*). Comp. Biochem. Physiol. Part D Genomics, Proteomics, **1**: 328–343.

Lignot, J.-H., Helmstetter, C., and Secor, S.M. 2005. Postprandial morphological response of the intestinal epithelium of the Burmese python (*Python molurus*). Comp. Biochem. Physiol. Part A Mol. Integr. Physiol. **141**: 280–291. doi:10.1016/j.cbpb.2005.05.005.

MacKenzie, S., Cutler, C.P., Hazon, N., and Cramb, G. 2002. The effects of dietary sodium loading on the activity and expression of Na,K-ATPase in the rectal gland of the European dogfish (*Scyliorhinus canicula*). Comp. Biochem. Physiol. Part B Biochem. Mol. Biol. **131**: 185–200. doi:10.1016/S1096-4959(01)00493-6. PMID:11818240.

Newbound, D.R., and O'Shea, J. 2001. The microanatomy of the rectal salt gland of the Port Jackson shark, *Heterodontus portusjacksoni* (Meyer) (Heterodontidae): suggestions for a countercurrent exchage system. Cells Tissues Organs, **169**: 165–175. doi:10.1159/000047875. PMID:11399857.

Oguri, M. 1964. Rectal gland of marine and freshwater sharks: comparative histology. Science (Washington, D.C.), **144**: 1151–1152. doi:10.1126/science.144.3622.1151. PMID:17814499.

Olson, K.R. 1999. Rectal gland and volume homeostasis. *In* Sharks,

skates, and rays. *Edited by* W.C. Hamlett. Johns Hopkins University Press, Baltimore, Md. pp. 329–352.

Ott, B.D., and Secor, S.M. 2007. Adaptive regulation of digestive performance in the genus *Python*. J. Exp. Biol. **210**: 340–356. doi:10.1242/jeb.02626. PMID:17210969.

Perry, S.F. 1997. The chloride cells: structure and function in the gills of the freshwater fishes. Annu. Rev. Physiol. **59**: 325–347. doi:10.1146/annurev.physiol.59.1.325. PMID:9074767.

Piermarini, P.M., and Evans, D.H. 1998. Osmoregulation of the Atlantic stingray (*Dasyatis sabina*) from the freshwater Lake Jesup of the St. John River, Florida. Physiol. Zool. **71**: 553–560. PMID:9754532.

Pillans, R.D., and Franklin, C.E. 2004. Plasma osmolyte concentrations and rectal gland mass of bull sharks *Carcharhinus leucas*, captured along a salinity gradient. Comp. Biochem. Physiol. Part A Mol. Integr. Physiol. **138**: 363–371. doi:10.1016/j.cbpb.2004.05.006.

Pillans, R.D., Good, J.P., Anderson, W.G., Hazon, N., and Franklin, C.E. 2008. Rectal gland morphology of freshwater and seawater acclimated bull sharks *Carcharhinus leucas*. J. Fish Biol. **72**: 1559–1571. doi:10.1111/j.1095-8649.2008.01765.x.

Schmidt-Nielsen, K. 1959. Salt glands. Sci. Am. **200**: 109–116. PMID:13624738.

Shuttleworth, T.J., and Hildebrandt, J.P. 1999. Vertebrate salt glands: short- and long-term regulation of function. J. Exp. Biol. **283**: 689–701.

Shuttleworth, T.J., Thompson, J., Munger, S.R., and Wood, C.M. 2006. A critical analysis of carbonic anhydrase function, respiratory gas exchange, and the acid–base control of secretion in the rectal gland of *Squalus acanthias*. J. Exp. Biol. **209**: 4701–4716. doi:10.1242/jeb.02564. PMID:17114403.

Silva, P., and Epstein, F.H. 2002. Role of the cytoskeleton in secretion of chloride by shark rectal gland. J. Comp. Physiol. B, **172**: 719–723. PMID:12444471.

Silva, P., Solomon, R.J., and Epstein, F.H. 1997. Transport mechanisms that mediate the secretion of chloride by the rectal gland of *Squalus acanthias*. J. Exp. Zool. **279**: 504–508. doi:10.1002/(SICI)1097-010X(19971201)279:5<504::AID-JEZ14>3.0.CO;2-7. PMID:9392873.

Valentich, J.D., Karnaky, K.L., and Ecay, T.W. 1996. Ultrastructural and cytochemical characterization of cultured dogfish shark rectal gland cells. Am. J. Physiol. **271**: C1993–C2003. PMID:8997202.

Walsh, P.J., Kajimura, M., Mommsen, T.P., and Wood, C.M. 2006. Metabolic organization and effects of feeding on enzyme activities of the dogfish shark (*Squalus acanthias*) rectal gland. J. Exp. Biol. **209**: 2929–2938. doi:10.1242/jeb.02329. PMID:16857877.

Wood, C.M., Pärt, P., and Wright, P.A. 1995. Ammonia and urea metabolism in relation to gill function and acid–base balance in a marine elasmobranch, the spiny dogfish (*Squalus acanthias*). J. Exp. Biol. **198**: 1545–1558. PMID:9319448.

Wood, C.M., Kajimura, M., Mommsen, T.P., and Walsh, P.J. 2005. Alkaline tide and nitrogen conservation after feeding in the elasmobranch *Squalus acanthias*. J. Exp. Biol. **208**: 2693–2705. doi:10.1242/jeb.01678. PMID:16000539.

Wood, C.M., Bucking, C.P., Fitzpatrick, J., and Nadella, S.R. 2007*a*. The alkaline tide goes out and the nitrogen stays in after feeding in the dogfish shark, *Squalus acanthias*. Respir. Physiol. Neurobiol. **159**: 163–170. doi:10.1016/j.resp.2007.06.008. PMID:17656159.

Wood, C.M., Kajimura, M., Bucking, C.P., and Walsh, P.J. 2007*b*. Osmoregulation, ionoregulation, and acid–base regulation by the gastrointestinal tract after feeding in the dogfish shark. J. Exp. Biol. **210**: 1335–1349. doi:10.1242/jeb.02736. PMID:17401117.

Wood, C.M., Munger, S.R., Thompson, J., and Shuttleworth, T.J. 2007*c*. Control of rectal gland secretion by blood acid–base status in the intact dogfish shark (*Squalus acanthias*). Respir. Physiol. Neurobiol. **156**: 220–228. doi:10.1016/j.resp.2006.09.003. PMID:17049933.

Wood, C.M., Kajimura, M., Mommsen, T.P., and Walsh, P.J. 2008. Is the alkaline tide a signal to activate metabolic or ionoregulatory enzymes in the dogfish shark (*Squalus acanthias*)? Physiol. Biochem. Zool. **81**: 278–287. doi:10.1086/587094. PMID:18419554.

Zeidel, J.D., Mathai, J.C., Campbell, J.D., Ruiz, W.G., Apodaca, G.L., Riordan, J., and Ziedel, M.L. 2005. Selective permeability barrier to urea in shark rectal gland. Am. J. Physiol. **289**: F83–F89.